IMPROVEMENTS TO THE ACCURACY OF DISCHARGE MEASUREMENTS BY ACOUSTIC SCINTILLATION RESULTING FROM REVISIONS TO DATA PROCESSING PROCEDURES

D.D. Lemon,
ASL AQFlow Inc., Victoria, BC, Canada,

D. R. Topham,
Topham Scientific Consulting, Victoria, BC, Canada

D. Billenness,
ASL AQFlow Inc., Victoria, BC, Canada

ABSTRACT

A number of changes have been made recently to improve the algorithms used for processing acoustic scintillation data for turbine discharge measurements, as a result of ongoing research into the factors affecting the accuracy of the method. These improvements are based on the results from a number of applications of the Acoustic Scintillation Flow Meter over the past two years, and encompass changes to both the instrument operation and the time series data processing. The effect of these changes is illustrated through a re-analysis of the data from acoustic scintillation flow measurements made in 2004 at Lower Granite Dam, a large, low-head plant on the Snake River in Washington State. Acoustic time-of-travel measurements in the intake and Winter-Kennedy differential pressure measurements were made at the same time. The effect of the revisions on comparisons to the other measurements and model predictions is discussed in detail. The improved procedures were used in a recent blind comparison test of intake flow measurement methods against a code-accepted reference (in the penstock) performed at BC Hydro's Kootenay Canal generating station. Agreement to within 0.5% between the acoustic scintillation and reference methods was found, with no significant dependence on flow speed. These results show that, under conditions typical of a low-head intake, flow measurement by acoustic scintillation can achieve the absolute accuracy required by the ASME and IEC test codes.

1. ACOUSTIC SCINTILLATION PRINCIPLES AND IMPLEMENTATION

The Acoustic Scintillation Flow Meter (ASFM) uses a technique called acoustic scintillation drift [1, 2] to measure the flow velocity perpendicular to a number of acoustic paths established across the intake to the turbine. Short (16 μsec) pulses of high-frequency sound (307 kHz) are sent from transmitting arrays on one side to receiving arrays on the other, at a rate of approximately 250 pings /second. Fluctuations in the amplitude of those acoustic pulses result from turbulence carried along by the flow. The ASFM measures those fluctuations (known as scintillations) and from them computes the lateral average (i.e. along the acoustic path) of the velocity perpendicular to each path.

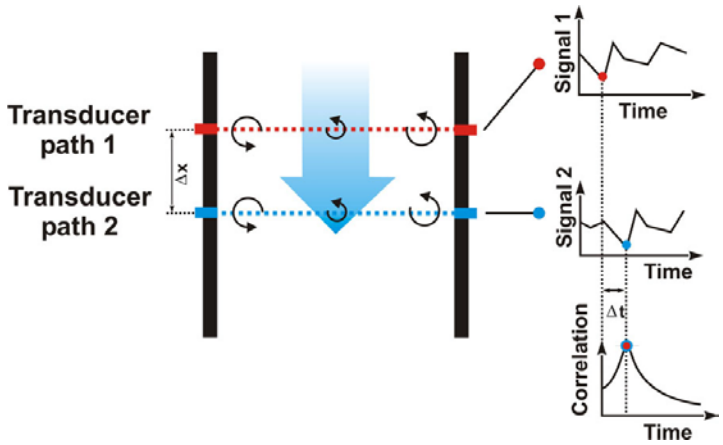

Fig. 1: Schematic representation of acoustic scintillation drift.

The ASFM utilizes the natural turbulence embedded in the flow, as shown in Fig. 1. In its simplest form, two transmitters are placed on one side of the measurement section, two receivers at the other. The signal amplitude at the receivers varies randomly as the turbulence along the propagation paths changes with time and the flow. If the two paths are sufficiently close (Δx), the turbulence remains embedded in the flow, and the pattern of these amplitude variations at the downstream receiver will be nearly identical to that at the upstream receiver, except for a time delay, Δt. This time delay corresponds to the peak in the time-lagged cross-correlation function calculated for Signal 1 and Signal 2. The mean velocity perpendicular to the acoustic paths is then $\Delta x/\Delta t$. Using three transmitters and three receivers at each measurement level allows both the magnitude and inclination of the velocity to be measured. The ASFM computes the discharge through each bay of the intake by integrating the horizontal component of the velocity over the cross-sectional area of the intake. In a multi-bay intake, the discharges through each bay are summed to compute the total discharge. An overview of the discharge computation procedure may be found in [3] and [4].

The ASFM instrument consists of five major components: transmitting (Tx) and receiving (Rx) transducers and underwater cabling, switching canisters, surface connection cables, a data acquisition Surface Unit, and a PC computer with the user interface for controlling and operating the ASFM (ASFM Link software). The ASFM typically is divided into 3 groups for operation in multi-bay intakes; each group consists of a set of transducers (in pairs of Tx and Rx), two switching canisters, and cabling. A single ASFM system can have up to 30 paths with 3 groups (10 paths per bay typically in a 3-bay intake – Fig. 2). One path from each group may be sampled simultaneously, provided the path lengths are equal.

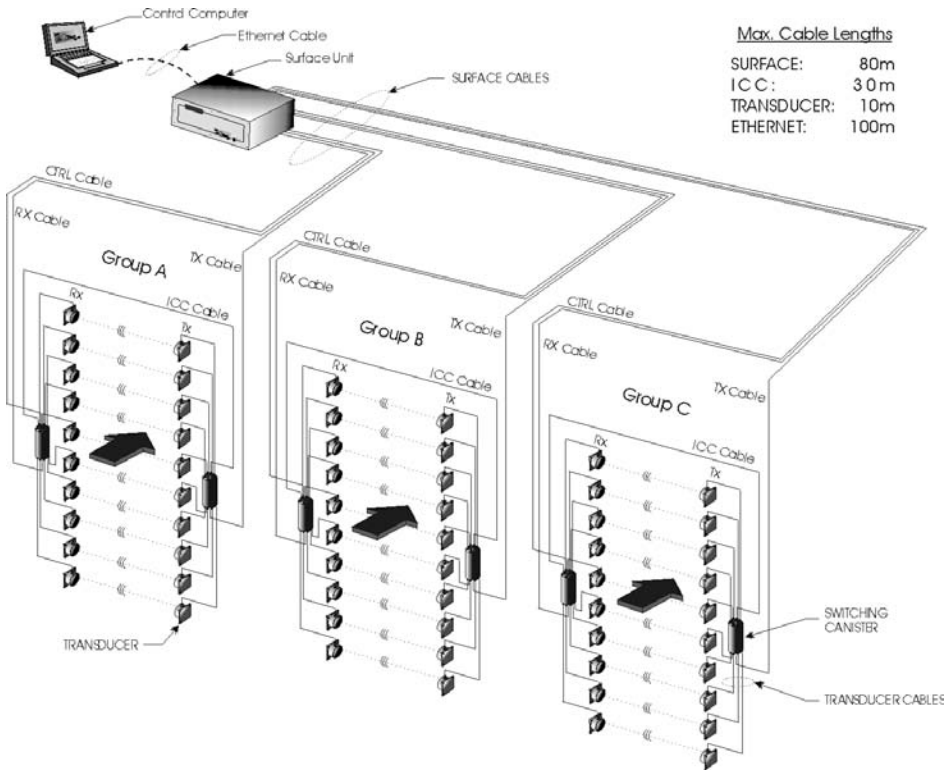

Figure 2: Components of a typical multi-bay ASFM.

Typically, the ASFM sensors are installed on frames which are placed in the stoplog slots of each bay; the frames are designed so that the transducer faces sit flush with the sidewalls of the intake (Fig. 3).

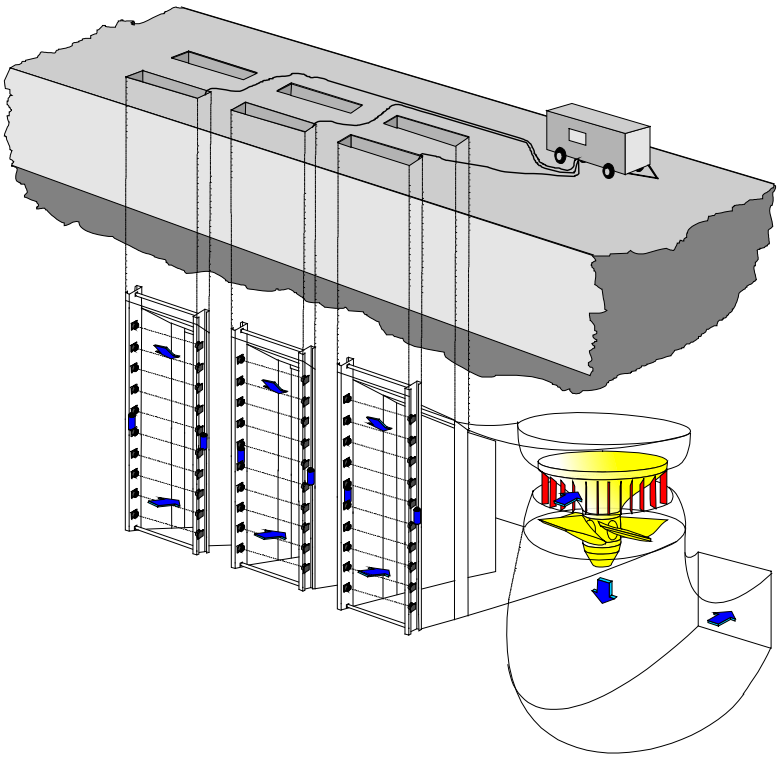

Figure 3: Typical ASFM installation in a 3-bay intake

2. DATA PROCESSING ALGORITHM CHANGES

Improvements have been made in both the ASFM's operating and data processing software. The operational change is an improvement to the signal detection and locking procedure that reduces the probability of selecting reflected-path signals. Changes have been made in two parts of the data processing algorithm: the filtering applied to the time series, and the method by which the results from the individual blocks within the time series are combined to compute the flow velocity.

2.1 Operating Procedure Changes

Accurate measurement of flow velocity by acoustic scintillation requires that the fluctuations in the received signal amplitude be caused entirely by the effects of the refractive-index turbulence along the propagation path across the intake. Signal fluctuations can also arise from vibration in the mounting frame or by interference from signals arriving over paths other than directly between the transmitter and receiver. The frame and intake sidewalls are generally good acoustic reflectors, and as a result signals can be reflected multiple times across the intake before dying away. At the high ping rates used by the ASFM (nominal 250 Hz on each of 3 elements in the transducer arrays) interference by signals from preceding pings is quite possible. The operating software includes a procedure to calculate whether reflected signals from up to 12 previous pings would overlap the current direct arrival, and to adjust the pinging rate to avoid that. This procedure previously depended on computing the signal travel time from the measured path length and water temperature, and hence was vulnerable to changes in the temperature or errors in its measurement.

A modification has been made to allow direct measurement of the signal travel time by temporarily reducing the ping rate to 10 Hz, so that no reflections from previous pings are present, and directly measuring the arrival time of the signal for each path. The accurate travel time ensures that the correct arrival is recorded, and that the ping rate adjustment to avoid multi-path interference is correct.

2.2 Acoustic Time Series Filtering

The raw acoustic amplitude time series used in the acoustic scintillation method are band-pass filtered before computing the cross-correlations used to calculate the velocity. The original filtering procedure used a fixed value of 40 Hz for the upper limit to the passband, while the lower limit was selected using an iterative procedure. The lower cut-off was varied between 0.5 Hz and 15.5 Hz in steps of

1 Hz. The velocity was computed for each selection, and the selection which gave the highest quality index was used for the reported velocity. The time series was divided into 2048-point blocks, with a velocity computed for each block. Outliers from that set of velocities were rejected using the Grubbs T-statistic [5], and the velocity used in the discharge was then the average of the individual velocities of the remaining blocks. The quality index is the product of the mean peak cross-correlation score multiplied by the fraction of the blocks that were retained.

The revised procedure addresses limitations arising from the fixed range over which the lower passband limit was chosen, and also modifies the way the correlation results are used to compute the velocity. The turbulence that produces the acoustic scintillations occupies a fixed range of spatial scales; the range of frequencies it produces in the acoustic time series therefore varies with the mean flow speed. The previous procedure did not account for this effect, and therefore was not always properly aligned with the wavenumbers producing the scintillations. The passband selection procedure has been modified to address that limitation. The passband frequency limits are selected from one of five sets, designed to maintain the same wave number range in the turbulence as the source of the amplitude fluctuations. An initial estimate of the flow velocity computed from data filtered with a fixed passband of 6.5 to 40 Hz is used to select the passband limit set; the upper limit of each set is fixed, and the lower limit is selected from a range of frequencies specific to each set. The selection is an iterative process; the lower limit frequency, f_L, is incremented in steps from the minimum to the maximum of the range for the first few blocks of data. The ranges and step sizes are shown in the table below:

Table 1: Filtering passband limits.

Initial Velocity Estimate (m/s)	Upper Band Limit (Hz)	Range for Selection of Lower Band Limit (Hz)	Frequency Step Size (Hz)
V < 1.5	40	1 - 7	0.5
1.5 $\leq$ V < 2.5	45	2 - 14	1
2.5 $\leq$ V < 3.5	50	3 - 21	1.5
3.5 $\leq$ V < 4.5	55	4 - 28	2
4.5 $\leq$ V < 6.0	60	5 - 35	2.5

The peak cross correlation values for the three pairs of time series for each block are recorded, and those above a threshold value of 0.2 (the theoretical minimum) are retained. A quality index, QI, is then computed as the product of the ratio of the average peak correlation score for each pair to the theoretical maximum and the fraction of the scores that were retained as being above the threshold value. The procedure is repeated for each value of f_L, and the value with the highest QI is used to filter the entire data set.

2.3 Velocity Calculation

Previously, a velocity was computed for each 2048-point data block in the acoustic time series. If one or more of the individual pair correlation scores were below the threshold, the entire block was rejected. The procedure has been revised to retain blocks wherein only some of the pair correlation scores were above the threshold, and then the average of all the retained scores and their times is computed for each pair. The velocity is computed from their averages, after rejection of outliers. Outliers were rejected using the Grubbs T-statistic [5]. For example, in a 6 block set, values more than 1.89 standard deviations from the mean are removed. The quality index QI is recomputed after outlier rejection. The uncertainty for the velocity is computed as

$$\Delta v = \frac{\sigma}{\tau_{av}}$$

where τ_{av} is the average time delay over the N blocks for the pair of elements with the highest peak cross- correlation score (they are the most closely aligned with the flow direction) and σ is its standard deviation. The random error may be further reduced by making replicate runs and averaging them together.

3. RESULTS FROM LOWER GRANITE DAM

The effect of these changes is illustrated through a re-analysis of the data from acoustic scintillation flow measurements made in 2004 at Lower Granite Dam, a large, low-head plant on the Snake River in Washington State. Acoustic time-of-travel measurements in the intake and Winter-Kennedy differential pressure measurements were made at the same time. The intakes to the turbines are equipped with fish diversion screens (referred to as ESBS), and flows were measured with and without the screens in place. The screens, which consist of a rectangular array of small bars, are inserted into each bay of the intake at an angle to divert part of the flow, and with it juvenile salmon migrating downstream, into a bypass conduit around the turbine. They cause a significant distortion of the flow field in the intake, as may be seen in Figure 4.

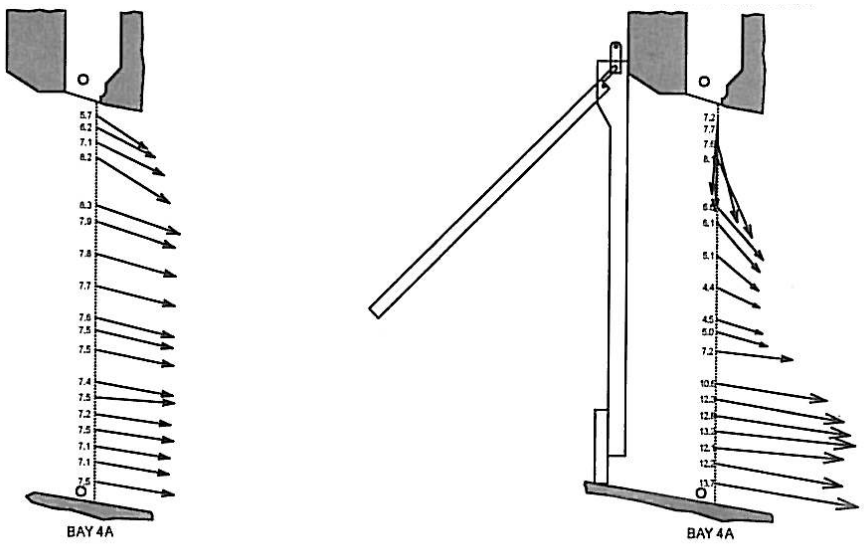

Figure 4: Flow field in one bay of the Lower Granite intake, without screens (left) and with screens (right).

Comparisons with the results of other measurement methods used and with model predictions may be found in [6], where the acoustic scintillation flow data pre-date the data processing improvements discussed above. All the ASFM data were reprocessed with the updated algorithms, which will be referred to as version 2.57 (V2.57). Plots of the revised vs. original flows are shown in Figures 5 and 6 for the screens-out and screens-in cases, respectively. The difference is small for the screens-out cases, being on average a 0.4% increase, showing no trend with discharge in the fractional difference. With screens in however, the difference is greater, ranging from 0.9% at the minimum discharge to 3.0% at the maximum discharge and averaging 2.0%.

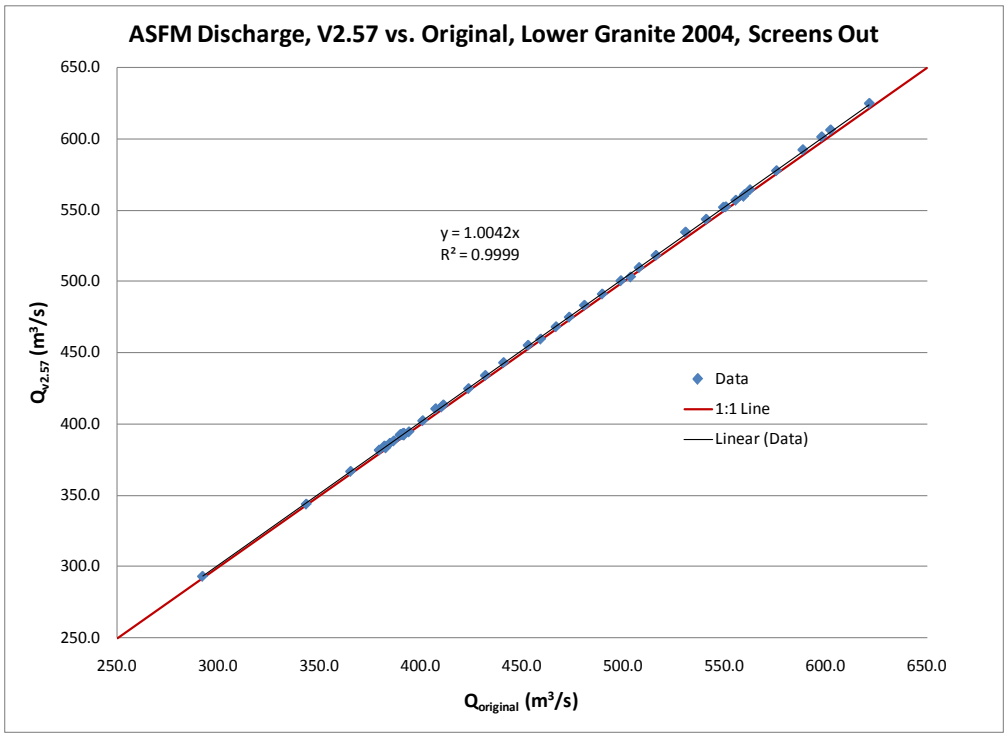

Figure 5: Revised (V2.57) ASFM discharge vs. original, all screens-out runs.

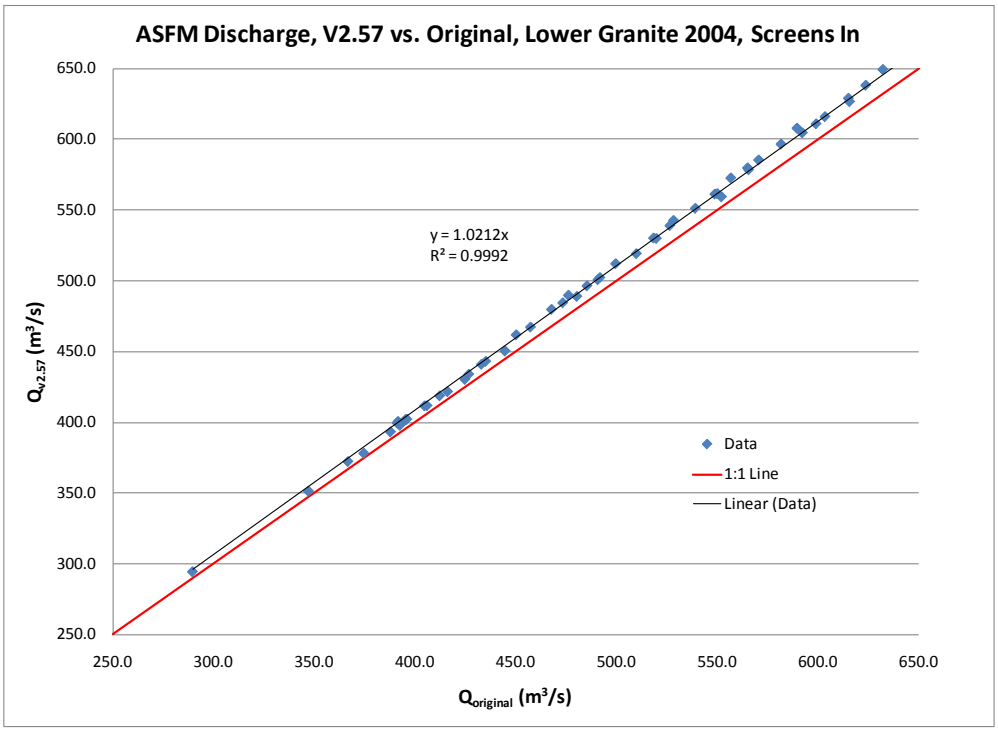

Figure 6: Revised (V2.57) ASFM discharge vs. original, all screens-in runs.

In comparison with the flows measured by the intake time-of-travel instrument discussed in [6], the average difference between the ASFM and the time-of-travel flows for all off-cam runs is reduced to 0.8% from 1.2% with screens out (the value of 1.6% in [6] is an approximation, and is not quite correct), and to 2.0% from 3.9% with screens in. The efficiency curve for operation without screens computed from the ASFM data shown in [6] therefore shifts down by 0.4%, placing it about 1% below the model curve and 0.5% above the curve derived from the time-of-travel data. With screens in, the efficiency curve computed from the ASFM data moves down by 0.8% at low flows and 2.5% at high flows, which aligns it close to the

curve derived from the Winter-Kennedy data, about 1.5% below the model curve and 1% above the curve derived from the time-of travel data.

Figure 7 illustrates the effect of the revised processing on the velocity field in the intake.

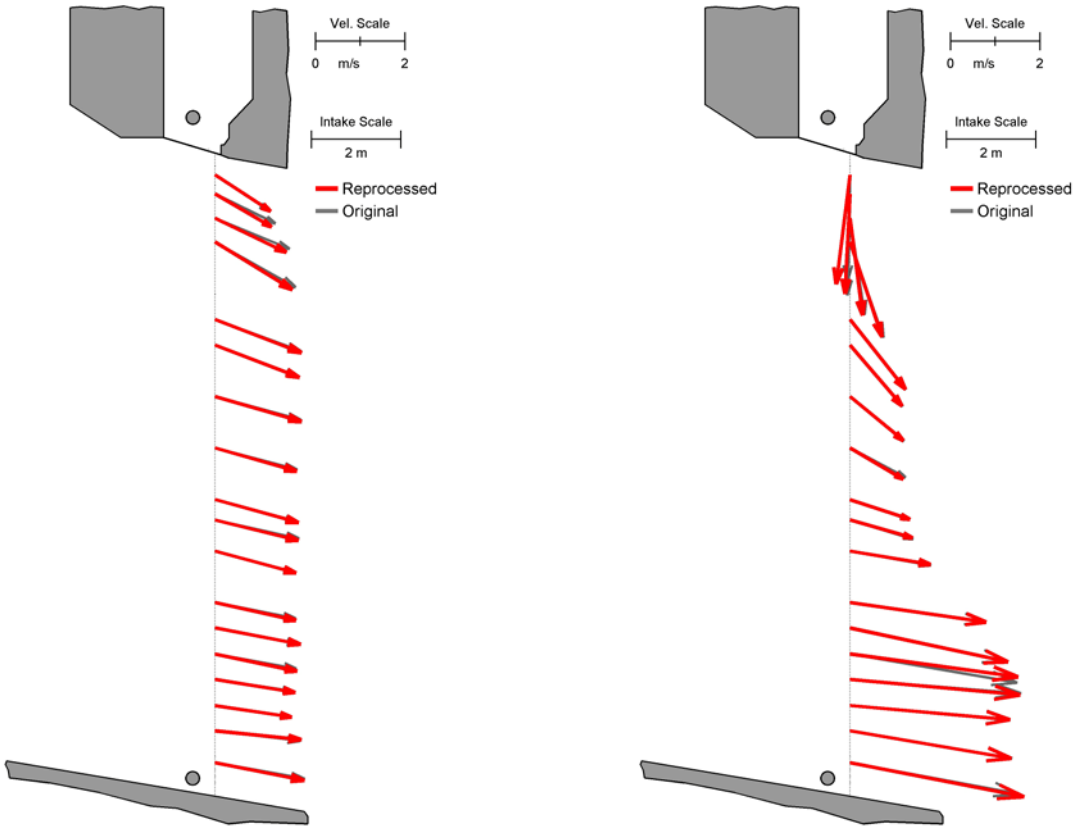

Figure 7: Laterally-averaged velocity vectors for Bay A, showing original(grey) and V2.57 processing (red), without ESBS (left panel) and with ESBS (right panel). (Off-cam, 24° blade, 80% servo).

The revised processing was also applied to a set of closely-spaced measurements (made previously at Lower Monumental Dam, another low-head plant on the Snake River of almost identical design) used to determine the form of the upper and lower boundary layers. There was no change in the upper layer, but the form of the lower layer (which is influenced by the presence of the frame's bottom cross-member) changed from $z^{-0.37}$ to $z^{-0.26}$. The revised processing produced only very small changes in the velocity vectors with no screens in place; most of the increase in the discharge arises from the change to the bottom boundary layer. With ESBS in place, there is an increase in the magnitude of the lowermost vector. Because of the greater velocity in the lower part of the intake caused by the presence of the screens, that increases the discharge by approximately 1%, with most of the remainder of the increase being in the bottom boundary layer (which is proportionately larger because of the higher velocity in the lower part of the intake).

Another comparison made in [6] is between the measured reduction in the power produced at fixed blade angles and servo settings with ESBS in place and the corresponding difference in calculated efficiency for each of the flow measurement methods. Figure 8 reproduces those comparisons (estimated from Figure 12 in [6]) and includes the revision to the efficiency difference for the ASFM data resulting from reprocessed discharge values. The data in [6] were plotted against the equivalent on-cam blade and gate setting for each of the fixed-blade power-loss curves; the revised ASFM discharges and resulting efficiencies were computed from the fixed blade data at the nearest measured setting to the on-cam position, and therefore may not be exactly equivalent. However, as Figure 8 shows, the effect is to raise the efficiency loss as measured by the ASFM from approximately 2.5% to approximately 3.5%, bringing it into closer agreement with the loss computed from the time-of-travel data. The differences between them are now 1% or less, and both exceed the power-loss values.

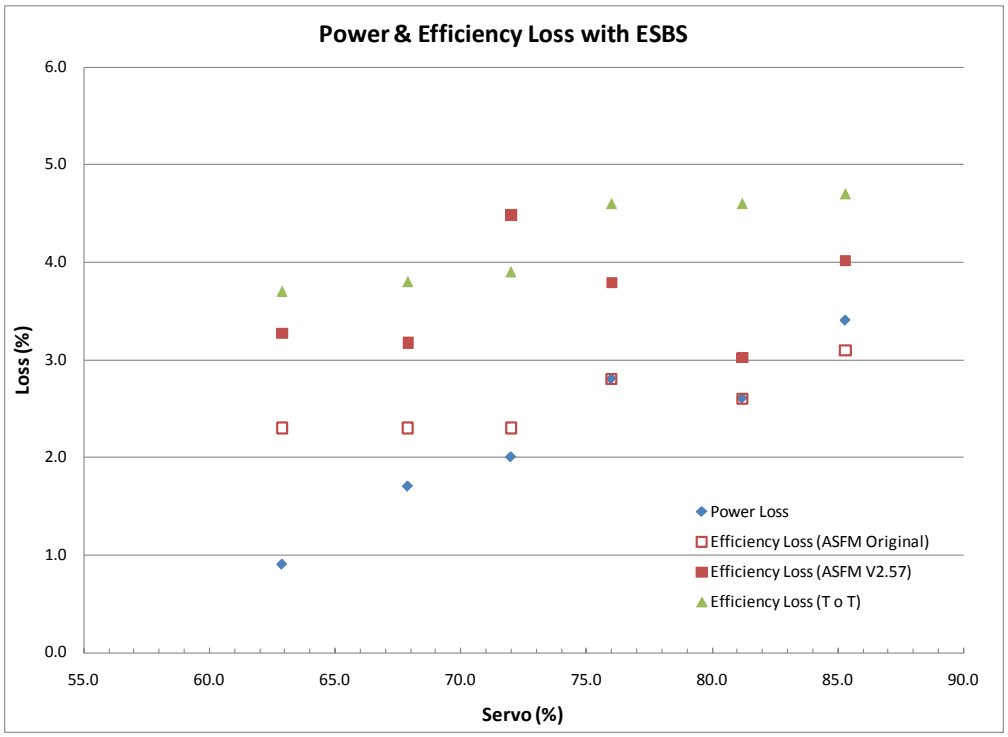

Figure 8: Power and efficiency loss comparison for original and V2.57 processing (power loss, ASFM original and Time-of-Travel efficiency changes estimated from Figure 12 in [6]).

4. KOOTENAY CANAL COMPARISON TESTS

In October 2009, acoustic scintillation was one of three intake flow measurements methods used in a blind comparison test at BC Hydro's Kootenay Canal plant, sponsored by CEATI (the Centre for Energy Advancement through Technological Innovation) and supervised by the PTC-18 Committee of the ASME. Kootenay Canal is a medium-head plant, with straight penstocks of sufficient length to meet code requirements for flow measurements in the penstock. Its intakes, however, are configured identically to those found in a typical low-head, short-intake plant, thereby making it an ideal site to test intake flow measurement methods, as a reference flow was provided by an acoustic time-of-travel instrument installed in a code-approved location in the penstock. The other two intake methods tested were current meters and acoustic time-of travel. None of the participants had knowledge of the reference or other discharges until after all final results were submitted to the test chief 30 days after completion of the tests. The acoustic scintillation measurements are reported in detail in [4].

The revisions to the data processing procedure and operating software described above were implemented in the ASFM used in the Kootenay Canal tests. Repeated runs were made at three flow rates characteristic of low-head intakes: nominal values of 1, 2 and 3 m/s average flow speed. Each of the conditions was repeated 12 times; the overall average fractional difference between the ASFM discharges and the reference discharge was +0.45%, with a standard deviation of 0.20%. Table 2 below lists the differences and standard deviations for each flow condition.

Nominal Intake Flow Speed (m/s)	Average Difference ASFM-Ref (%)	Standard Deviation (%)
1.0	0.51	0.25
2.0	0.46	0.18
3.0	0.38	0.15

Table 2: Summary of ASFM differences with reference flow at Kootenay Canal

In all cases the difference is well below the accepted uncertainty limits of the reference flow, with a slight decrease in both it and the standard deviation with flow speed. An additional set of tests was

performed during which the operation of the neighbouring units was varied, which showed no measurable effect on the accuracy of the ASFM discharge measurement from those variations.

5. CONCLUSIONS

Significant improvements in the precision and accuracy of the discharge measured by the ASFM have resulted from the recent improvements to the operating software and data analysis procedures. Re-analysis of data collected at Lower Granite Dam in 2004 illustrates that the improvements are greatest in poor hydraulic conditions, such as those introduced by the presence of fish diversion screens, which significantly perturb the flow field. Under well-behaved hydraulic conditions in the intake, the improvements are minor. Similar re-analyses are planned for ASFM data that has been collected at other plants on the Snake and Columbia Rivers where fish diversion screens are used.

The results of comparative testing against a code-approved reference flow measurement in the penstock at Kootenay Canal have shown that, under conditions typical of a low-head intake, flow measurement by acoustic scintillation can achieve the absolute accuracy required by the ASME and IEC test codes.

REFERENCES

1. Clifford, S.F. and D.M. Farmer, 1983. Ocean flow measurements using acoustic scintillation. J. Acoust. Soc. Amer., 74 (6). 1826-1832.
2. Farmer, D.M. and S.F. Clifford, 1986. Space-time acoustic scintillation analysis: a new technique for probing ocean flows. IEEE J. Ocean. Eng. OE-1 1(1), 42 – 50.
3. Lemon, D. D. and P. W. W. Bell, 1996. Measuring hydraulic turbine discharge with the Acoustic Scintillation Flow Meter. Proc. IGHEM, Montreal, 1996.
4. Lemon, D. D. and D. Billenness, 2010. Acoustic scintillation flow measurements in the intake at Kootenay Canal power plant. Proc. Hydro 2010, Lisbon, October 2010.
5. International Electrotechnical Commission, 1991. Field acceptance tests to determine the hydraulic performance of hydraulic turbines, storage pumps and pump-turbines. International Electrotechnical Commission, Publ. IEC-6041, Geneva.
6. Wittinger, R., 2005. Absolute flow measurement in short intake large Kaplan turbines - results of comparative flow measurements at Lower Granite powerhouse. Proc. Hydro 2005, Villach, Austria.

ACKNOWLEDGEMENTS

The authors wish to thank the US Army Corps of Engineers staff at Lower Granite Dam and the Hydroelectric Design Center for their cooperation and assistance during the installation and operation of the ASFM at the plant. We also thank the Kootenay Canal Generating Station as well as the BC Hydro test personnel for their cooperation and assistance during the comparison tests at Kootenay Canal. ASL's participation in the comparison test was partially funded through CEATI International Inc. Agreement No. T092700-0358C.

THE AUTHORS

David Lemon, M.Sc., graduated in Physics (Oceanography) from the University of British Columbia, Vancouver, in 1975. He joined ASL AQFlow's parent company, ASL Environmental Sciences Inc. in 1978. He is currently President of ASL AQFlow Inc., Victoria, B.C., with responsibility for internal research and development. He has been responsible for the development of the acoustic scintillation method for hydroelectric applications.

David Topham PhD., graduated in Aeronautical Engineering from Loughborough College of Technology in 1959, joining A.V. Roe, Manchester. In 1965 he joined the Circuit Interruption Laboratory of the English Electric Co. Stafford to work on gas-blast switch gear, gaining a Ph.D from Loughborough University in 1970. In 1974 he joined the Institute of Ocean Sciences, Sidney BC, retiring in 1985. He is currently a private consultant.

David Billenness, M.A.Sc., graduated in Mechanical Engineering from the University of Victoria, British Columbia, in 1995 and has worked for ASL AQFLow's parent company, ASL Environmental Sciences since 1997. He currently heads the field flow measurement program associated with the ASFM.